Skin Disease Predication And Analyzing Using Naive Bayes Classification Algorithms

¹. Mrs. K. Shunmuga Priya, ². Dr.(Mrs) V. Selvi,

Abstract:-In modern times medicine, skin disorders are widely recognized as prevalent illnesses in the human population. Skin cancer is a life-threatening cancer that poses a significant public health problem, with early detection being crucial for effective treatment and survival. The Severity of skin cancer and the rapid count of affected people make it necessary to introduce an automatic detection scheme. Generally, analysing and identifying skin disease in a short time is the most complex and challenging task. Several machine learning (ML) methods are introduced to achieve this. However, still fulfilling the skin cancer diagnosis is not accomplished completely. To achieve this, we proposed a machine learning model using naive bayes with ROC to predict skin disease with maximum accuracy. The proposed naive bayes is based on similar features and classifies several stages. The performance obtained by the naive bayes is compared with ensemble classifiers and CNN with several evaluation metrics. The analysis shows that the accuracy attained by the proposed naive bayes is 98.5 % far better than the others in terms of classification and accuracy.

Keywords: skin disease, classification, prediction, Machine learning, skin cancer, naïve bayes.

1. Introduction

Skin cancer forms in the skin cells. Skin cancer represents a major public health issue, as it is among the three fastest-growing and life-threatening cancer categories [1].WHO estimates that skin cancer accounts approximately 33% of all cancer cases[2], and the Skin Cancer Foundation reports that this disease is on the surge[3]. People of Caucasian descent are prone to skin cancer[4]. When skin is exposed to the sun's harmful radiation it damages the skin cell DNA[5] resulting in rapid cell proliferation and causes skin cancer. It is possible for skin tumours to be benign as well as malignant. Benign tumours, such as seborrheic keratosis, cherry angiomas, dermatofibroma, skin tags, pyogenic granuloma, and cysts[6], are growths that do not propagate to other organs. Alternatively, malignant tumours such as cutaneous skin cancer expand and penetrate neighbouring tissues and organs. It can also uncontrollably transmit dead cells to other parts of the body. Some of the prevailing types of malignant skin tumours include basal cell carcinoma, squamous cell carcinoma, and malignant melanoma.

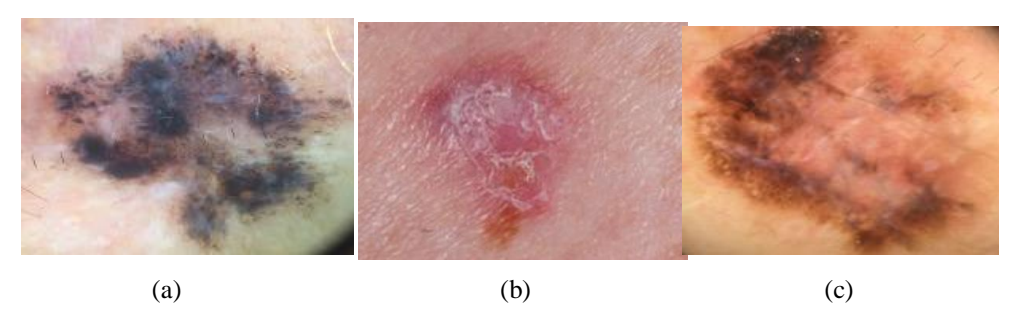


Figure 1. Principal types of malignant skin cancer (sources: and Dermatology Unit, Department of Clinical Internal Anesthesiologic Cardiovascular Sciences, "La Sapienza" University of Rome). (a) BCC. (b) SCC. (c) MM.

¹Research Scholar, Department of Computer Science, Mother Teresa Women's University, Kodaikanal.

²Assistant professor, Department of Computer Science, Mother Teresa Women's University, Kodaikanal

Basal cell carcinoma or basalioma (BCC) (Figure 1a). This type arises in the deepest epidermal cell known as the basal cell and this case accounts for approximately 80%. The slow growth rate of basal cells makes it treatable if it is detected and treated in a timely manner.

Squamous cell carcinoma or cutaneous spinocellular carcinoma (SCC) (Figure 1b). This type originates in the peripheral layer of the epidermis called the squamous cells. About 16% of cases arise from this category. If this case is detected and treated in time, it can be easily cured, otherwise it may spread and penetrate other organs.

Malignant Melanoma (MM) (Figure 1c)This is the most threatening type of skin tumour, occurring in the melanocytic cells of the epidermis. This kind arises 4% among the skin tumours and also persists with the mortality rate of 80%. The rapid growth of this tumour makes it hard to cure and is associated with a high mortality rate. A mere 14% of patients survive five years with metastatic melanoma after diagnosis. It is possible to cure 95% of patients who are diagnosed early which increases their chances of survival.

2. Related work

Many professionals and researchers proposed various classical network structures for using deep convolutional neural networks (DCNN) to classify skin lesions [7,8]. He et al [9] suggested a DL framework to address the issue of disintegration, which led to the creation of extended networks such as AlexNet [10], VGGNet, GoogLeNet [11], and Inception [12]. Whereas these network structures creates surplus parameters, which leads to model redundancy. DenseNet[13] avoids model redundancy by reusing features from earlier layers in the network. This network uses densely connected layers where each layer receives feature maps from all preceding layers. The VGG-16 network [14] investigated how the depth of a convolutional neural network affects its functioning. The process involves the repeated stacking of 3×3 convolution kernels and 2×2 max-pooling layers. The VGG-16 network's convolution sequence has limited attributes than a single convolution kernel but it has a larger nonlinear transformation than a one convolution layer. VGG-16 avoided enormous work in computational and complicated structure; it acquired many image features using fundamental network structure, compact convolutional kernels, and pooling layers.

Skin lesion classification based on multireceptive field: Here significant similarities are measured using advanced level traits whereas primary level traits such as edges and contours of pathological regions are capable of reflecting image content. Advancing these two traits will help to enhance the classification model[16]. Szegedy et al. [16] applied this method to skin lesion classification. This network is capable of analysing broad pathological regions when each convolution layer absorbs distinct weights—related to distinct fields. GoogleNet's [17] inception module constructed the respective field module using many convolution layers and various kernels surveying at the same centre. Multireceptive fields fetch premium features and strengthen their distinctiveness with the use of the object's spatial location and their surroundings.

In 2016, the International Skin Imaging Collaboration published the authentic ISIC archive [10] for the Biomedical Imaging (ISBI) challenge. This archive compiled various datasets from skin lesions, and it has undergone multiple changes over the years. Additionally, Kaggle has collected numerous databases associated with the ISIC archive, which data scientists and machine learners can use as a valuable resource for obtaining datasets.

The HAM10000 dataset, also known as the human-against-machine dataset[18](available at[19]), was gathered from two different resources: Cliff Rosendahl's skin cancer practice in Queensland, Australia, and the Dermatology Department of the Medical University of Vienna, Austria. This dataset, which comprises over 10,000 images with seven distinct diagnoses, was created by incorporating images to the ISIC2018 dataset.

The PH² database [20] (available at [21]) has 200 images. The images in this dataset are categorised into common nevi, atypical nevi, and melanoma skin cancer. It also contains elucidations like medical segmentation of the pigmented skin lesion, histological and clinical diagnoses, and other dermatological criteria scores. This database was obtained from the Dermatology Service of Hospital Pedro Hispano, Matosinhos, Portugal.

The MedNode dataset [22] (available at [23]) has the digital pictures of melanoma skin lesions and common nevus skin lesions. This dataset is acquired from the Department of Dermatology of the University Medical Center Groningen (UMCG).

Deep Learning-Based Skin Lesion Classification[24,25]. Gessert et al. [26] trained three neural network models before evaluating several techniques to balance their performance. They achieved an accuracy of 85.1% on ISIC2018 dataset classification and predicted with the use of a meta learning method. Shahin et al. [27] combined ResNet-50 and Inception-v3 network models to categorise seven skin lesions using an ensemble method. Its classification accuracy is higher than 89.9%. Amirreza et al. [28] investigated how image size impacts the classification of skin lesions using a pretrained CNN and transfer learning. They achieved 86.2%, a balanced multiclass accuracy on the testing set of the ISIC2018 classification challenge using multiscale and multi network models.

Al Masni et al. [29] used multiple convolutional network classifiers to classify lesion regions by segmenting pathological areas in their study. They achieved 89.28% classification accuracy with the ResNet-50 neural network which outperformed that of several other networks.

Zillur et al. [30] used five deep neural network models (ResNeXt, SeResNeXt, ResNet, Xception, and Dense-Net) to get the finest ensemble fusion. They obtained 88% classification accuracy with a weighted average ensemble learning-based model.

Abayomi-A et al. [31] oversampled data in a nonlinear lower-dimensional embedding manifold to create an image of synthetic melanoma. The larger images helped train the Squeeze Net deep learning model. Using DenseNet77, Nawaz, et al.[32] suggested a UNET model. They incorporated the DenseNet77 network to generate a comprehensive set of image characteristics at the encoder unit whereas the decoder unit segments the important points of computation.

3. Proposed methodology

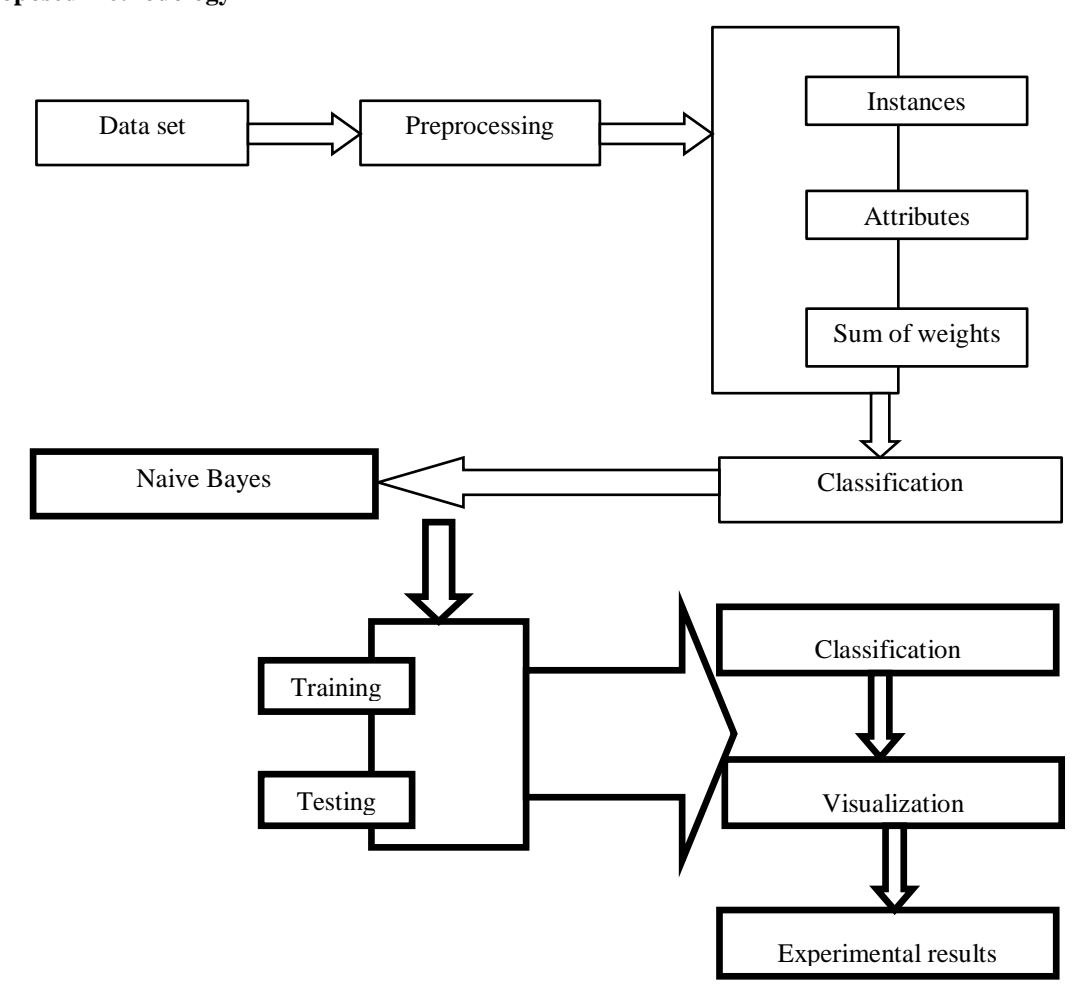


Figure 1: Proposed work

ISSN: 1001-4055 Vol. 44 No.6 (2023)

Data preprocessing

Data preprocessing is the primary and most essential step in creating a machine learning model, as it involves transforming raw data into a format that is suitable for use in the model. In the process of designing a machine learning project we have to get permission to clean. That is, before data is used in any activities, it must first be cleaned and formatted. Therefore this process is regarded as an important task.

Data set

The limited and insufficient variation of available dermatoscopic images for training neural networks presents a challenge for the automated diagnosis of pigmented skin lesions. To address this issue, we used the HAM10000 dataset ("Human Against Machine with 10000 training images"). In this study, we gathered dermatoscopic images from diverse populations using various acquisition methods. The resulting dataset provides training data for academic machine learning purposes, comprising 10,015 dermatoscopic images. The dataset includes a comprehensive selection of significant diagnostic categories, such as actinic keratoses and intraepithelial carcinoma / Bowen's disease (akiec), basal cell carcinoma (bcc), benign keratosis-like lesions (solar lentigines / seborrheic keratoses and lichen-planus like keratosis., bkl), dermatofibroma (df), melanoma (mel), melanocytic nevi (nv), and vascular lesions (angiomas, angiokeratomas, pyogenic granulomas, and haemorrhage, vasc). Almost 50% of the skin lesions were confirmed using histopathology (histo), while others were diagnosed through follow-up examination (follow_up), expert consensus (consensus), or confirmation by in-vivo confocal microscopy (confocal). The HAM10000_metadata file includes the lesion_id column, which tracks the images of multiple skin lesion datasets. The evaluation server continues to run (see the challenge website) though the test set is private. To ensure fair comparison of methods, publications that utilise the HAM10000 dataset for research purposes must evaluate their methods using the authorised test set provided by the dataset.

Tools used

The classification learner software trains the data classification models. This system enables experimentation using several classification methods with supervised machine learning. This data is capable of selecting features, analysing and training the models, explaining validation procedures and evaluating the results. Data can be analysed and machine learning models can be trained using various algorithms, such as support vector machines, naive Bayes, ensemble methods, neural network classification, discriminant analysis, kernel approximation, nearest neighbours, decision trees, and logistic regression. These algorithms can be automatically trained to find the best classification model for a given dataset by selecting relevant features and defining validation procedures to evaluate the model's accuracy. This process involves techniques such as cross-validation and feature selection, which help to ensure that the trained model is effective and not overfitting or underfitting the data. Overall, machine learning is a robust method for analysing and classifying data in an extensive selection of fields and applications. The supervised machine learning(labels or classes) can be spotted with upcoming and existing data effortlessly and the data is used to train the predicting model. We can either export the model to the workspace or create MATLAB code to reproduce the trained model, use it for new data, or gain further understanding about programmatic classification.

Naive Bayes

Naive Bayes is used to build classifiers. Vectors of attribute measures are used to assign class labels to distribute cases; these labels are obtained from a specific set. This applies a bunch of typical rile methodologies to train these classifiers. These Naive Bayes classifiers calculate certain attributes that are independent of other measurement attributes with class variables. This can be explained with an example: Let us consider a fruit to be examined, an apple which is typically red in colour, in the shape of a sphere with 10 cm width. The Naive Bayes classifier considers each of the attributes independently when estimating the probability that a fruit is an apple, without taking into account any potential correlations between the attributes such as colour, roundness, and diameter. This means that the classifier assumes that each attribute provides information about the probability of the fruit being an apple on its own, and that the attributes are not related to each other. While this assumption may not hold in reality, the Naive Bayes classifier is still a useful tool for classification tasks and has been shown to perform well in many real-world scenarios.

In real-time applications, maximum likelihood is often used to approximate parameters for Naive Bayes classifiers. However, it is possible to use Naive Bayes without employing Bayesian likelihood or techniques.

Despite their simple model and unrealistic assumptions, Naive Bayes classifiers have shown good performance in many complex real-world scenarios. The 2004 investigation of the Bayesian characterization issue, which pertains to the naive Bayes classifier's [5] independent assumptions about features, concluded that despite their implausibility in reality, naive Bayes classifiers can still be effective in some cases due to strong theoretical justifications. Example: navie bayes [6].

4. Experimental results

Recall

Recall can be calculated by the ratio of true positive examples to the sum of true positive and false negative examples. When the FN (false negatives) value is at its minimum and the recall value is high, it indicates that the examples were accurately recognized by the classifier.

$$Recall = \frac{TP}{TP + FN}$$

Precision

Precision is a matrix that calculates the proportion of correctly classified positive samples out of all predicted positive samples. A high precision value indicates positive results. The precision value is calculated by dividing the number of correctly classified positive samples by the total number of predicted positive samples.

$$Precision = \frac{TP}{TP + FP}$$

F-measure

The F-measure is calculated by combining the Recall and Precision. It is measured with the Harmonic Mean instead of the Arithmetic Mean, as the Harmonic Mean is more effective for high values. The F-measure values are always lower than both Recall and Precision. The calculation for F-measure is as follows:

$$F-measure = \frac{2*Recall*Precision}{Recall+Precision}$$

Scatter plot

A scatter plot is a visual representation that uses Cartesian coordinates to display the relationship between two variables. The plot is created from collected data and is typically shown as a figure. It consists of two axes, where the horizontal axis represents the values of one variable, and the vertical axis represents the values of the other variable. The data points are represented on the plot using different symbols, such as shapes, colours, or sizes.

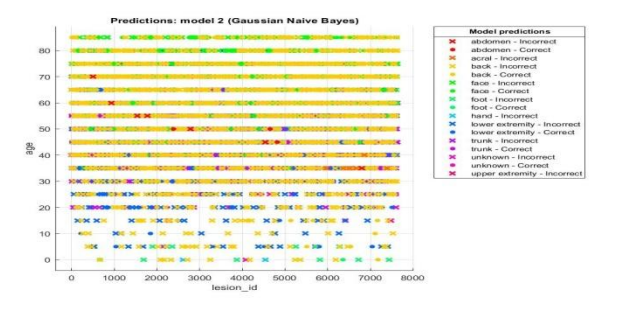


Figure:2 scatter plot lesion-id vs age

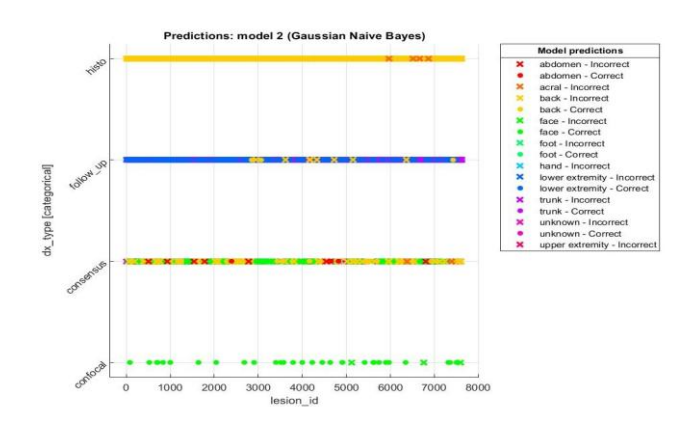


Figure:3 scatter plot lesion-id vs dx-type

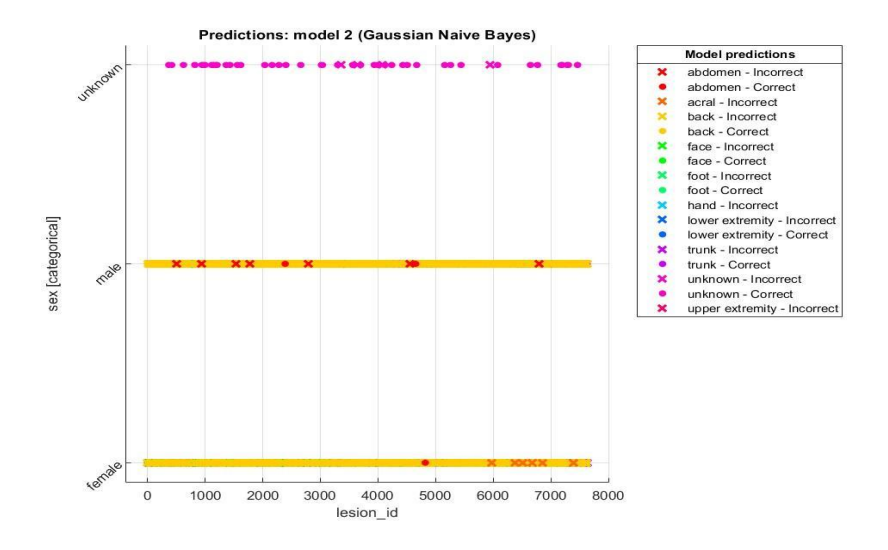


Figure: 4 scatter plot lesion-id vs sex

The above figures 2,3 and 4 illustrate the scatter plot lesion graphs compared with age, dx-type, and sex gathered from model 2 gaussian naive Bayes. In all three graphs lesion id is plotted on the x-axis with the range from 0 to 8000. In figure 2 the y-axis consists of all age groups from 1 to 100. In figure:3 dx-type are plotted in the y-axis with histopathology, follow-up examination, expert consensus (consensus), and confocal microscopy (confocal). In figure:4 the y-axis is plotted with sexual orientation like male, female, and unknown.

ROC

Machine learning is an effective approach to classification, but it's crucial to ensure that the performance of the applied model is adequate. After building the model, various evaluation metrics are used to assess its performance. Among these metrics, the most important one for measuring the classification model's performance is the AUC-ROC(Area Under the Receiver Operating Characteristic Curve) curve. This curve is widely used to evaluate classification accuracy, and the results obtained from the proposed model are displayed in the form of an AUC-ROC curve. This curve gets insight into the model's performance and identifies areas where it may need to be improved.

Vol. 44 No.6 (2023)

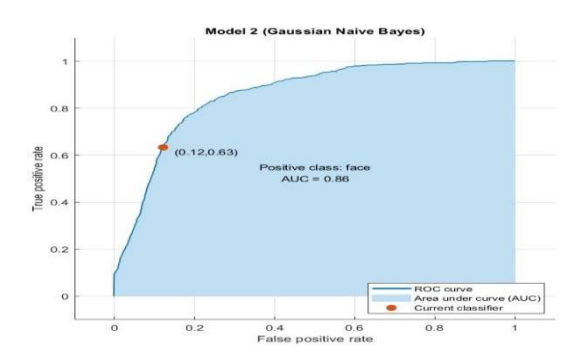


Figure:5 ROC in face

Figure 5 represents the ROC(Receiver Operating Characteristic Curve) obtained from Gaussian Naive Bayes with face. The X- axis is plotted with the false positive rate ranging from 0 increasing with the variation of 0.2 until 1 and the Y-axis contains true positive rates. In this graph dark blue coloured line indicates the range of ROC curve, light blue shaded area denotes AUC(Area under curve), and red dot represents current classifier. Here the AUC value of face is 0.83.

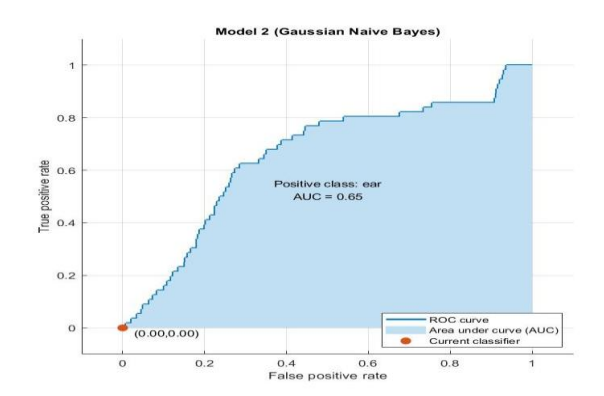


Figure:6 ROC in ear

Figure 6 represents the ROC(Receiver Operating Characteristic Curve) obtained from Gaussian Naive Bayes with ear. The X- axis is plotted with the false positive rate ranging from 0 increasing with the variation of 0.2 until 1 and the Y-axis contains true positive rates. In this graph dark blue coloured line indicates the range of ROC curve, light blue shaded area denotes AUC(Area under curve), and red dot represents current classifier. Here the AUC value of face is 0.65.

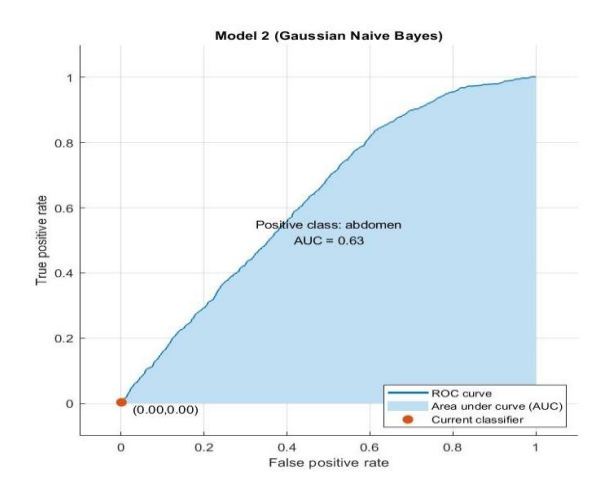


Figure: 7 ROC abdomen

Figure 7 represents the ROC(Receiver Operating Characteristic Curve) obtained from Gaussian Naive Bayes with abdomen. The X- axis is plotted with the false positive rate ranging from 0 increasing with the variation of 0.2 until 1 and the Y-axis contains true positive rates. In this graph dark blue coloured line indicates the range of ROC curve, light blue shaded area denotes AUC(Area under curve), and red dot represents current classifier. Here the AUC value of abdomen is 0.63.

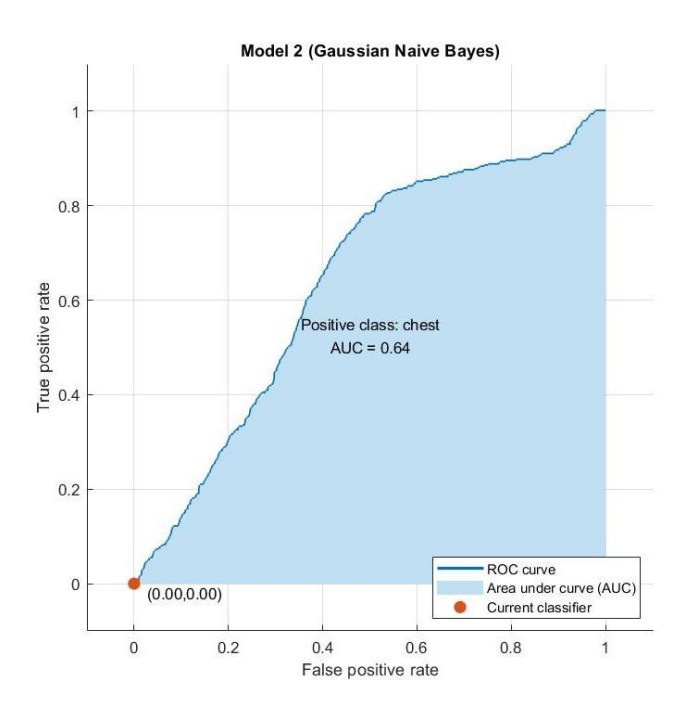


Figure:8 ROC chest

Figure 8 represents the ROC(Receiver Operating Characteristic Curve) obtained from Gaussian Naive Bayes with chest. The X- axis is plotted with the false positive rate ranging from 0 increasing with the variation of 0.2 until 1 and the Y-axis contains true positive rates. In this graph dark blue coloured line indicates the range of ROC curve, light blue shaded area denotes AUC(Area under curve) , and red dot represents current classifier. Here the AUC value of the chest is 0.64.

Confusion matrix

A confusion matrix displays the outcomes of a classification problem, showing two types: correct prediction and incorrect predictions. This information is represented through a breakdown and count values, determining the specific types of errors that the classifier is making and how these errors are occurring, which can then inform improvements to the model or adjustments to the data.

Description of the Terms

- Positive (P): Observation is positive
- Negative (N): Observation is not positive
- True Positive (TP): Observation is positive and is predicted to be positive.
- False Negative (FN): Observation is positive but is predicted negative.
- True Negative (TN): Observation is negative and is predicted to be negative.
- False Positive (FP): Observation is negative but is predicted positive.

Model 2 (Gaussian Naive Bayes) 555 16 abdomen back chest face genital hand remity scalp trunk upper extremity Predicted Class

Figure:8 confusion matrix for number of observations



Figure: 9 confusion matrix for TPR (true positive rate) and FNR (false negative rate)

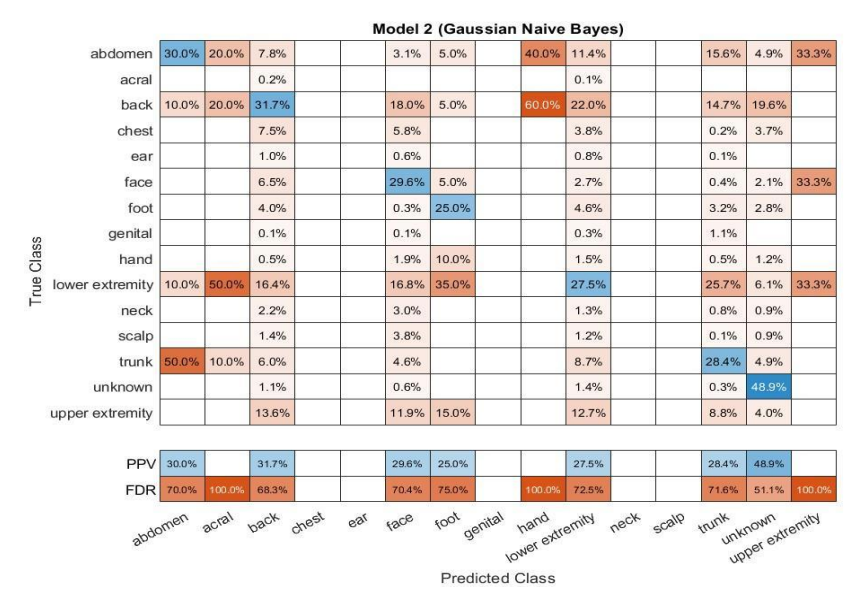


Figure: 10 confusion matrix PPV and FDR

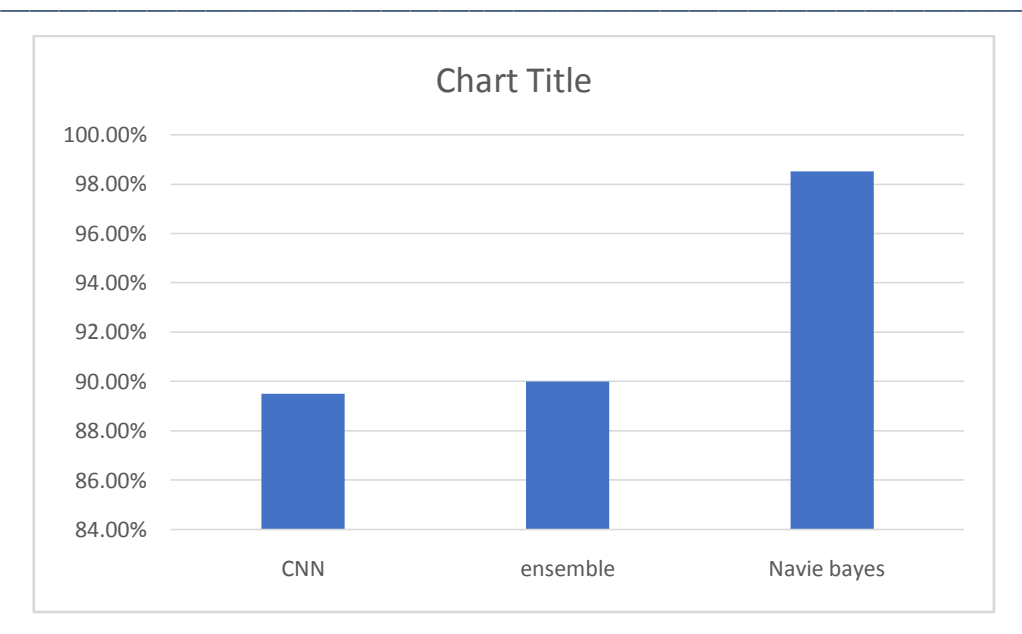


Figure:11 comparison bar graph of CNN, ensemble and navie bayes

Classification	Accuracy
CNN	89.5 %
ensemble	90%
Naive bayes	98.5%

The above figures 8,9,10 illustrate the performance of the proposed optimised naive bayes under a confusion matrix with the models. Figure 8,9,10 shows the obtained true class and predictive class from the models along with the number of observations, TPR and FNR, PPV and FDR. In the confusion matrix predicted classes are noted in columns, and true classes are noted in rows from the models. Table 3 shows the performance analysis of the prediction model between the SVM and Resnet with the proposed Ensemble. The overall accuracy is defined through the evaluation metrics which includes classification accuracy, Recall, precision, and F-measure. The proposed naive bayes achieves 98.5% accuracy, which is higher than the CNN and ensemble classifier.

5.Conclusion

This paper proposes a naive bayes with ROC for detecting skin cancer from the images. Automatic skin disease detection is very favourable for the patients affected with skin cancer. It helps the physician with more accuracy and can cure diseases at the beginning stage. In this work, we analysed the existing challenges and complexities in achieving the accurate, correct prediction from the images. The proposed approach applies multiple classifiers for handling huge data and employs resampling strategies to deal with the small amount of data. To analyse the performance of the proposed naive bayes classifier, a comparison work is carried out between the CNN and ensemble method. The evaluation metrics for comparison are classification accuracy, Recall, precision, and F-measure. The performance attained by the proposed naive bayes is more effective, especially in accuracy, than the others.

References

[1] Apalla, Z.; Nashan, D.; Weller, R.B.; Castellsagué, X. Skin Cancer: Epidemiology, Disease Burden, Pathophysiology, Diagnosis, and Therapeutic Approaches. Dermatol.Ther. 2017, 7 (Suppl. 1), 5–19. [CrossRef] [PubMed]

- [2] Hu, W.; Fang, L.; Ni, R.; Zhang, H.; Pan, G. Changing trends in the disease burden of non-melanoma skin cancer globally from 1990 to 2019 and its predicted level in 25 years. BMC Cancer 2022, 22, 836. [CrossRef] [PubMed]
- [3] Pacheco, A.G.; Krohling, R.A. Recent advances in deep learning applied to skin cancer detection. arXiv 2019, arXiv:1912.03280.
- [4] Goyal, M.; Knackstedt, T.; Yan, S.; Hassanpour, S. Artificial intelligence-based image classification methods for diagnosis of skin cancer: Challenges and opportunities. Comput.Biol. Med. 2020, 127, 104065. [CrossRef] [PubMed]
- [5] Narayanan, D.L.; Saladi, R.N.; Fox, J.L. Ultraviolet radiation and skin cancer. Int. J. Dermatol. 2010, 49, 978–986. [CrossRef]
- [6] Hasan, M.R.; Fatemi, M.I.; Khan, M. M.; Kaur, M.; Zaguia, A. Comparative Analysis of Skin Cancer (Benign vs. Malignant) Detection Using Convolutional Neural Networks. J. Healthc. Eng. 2021, 2021, 5895156. [CrossRef]
- [7] Al-Masni, M.A.; Al-Antari, M.A.; Choi, M.-T.; Han, S.-M.; Kim, T.-S. Skin lesion segmentation in dermoscopy images via deep full resolution convolutional networks. Comput. Methods Programs Biomed. 2018, 162, 221–231. [CrossRef]
- [8] Dildar, M.; Akram, S.; Irfan, M.; Khan, H.U.; Ramzan, M.; Mahmood, A.R.; Alsaiari, S.A.; Saeed, A.H.M.; Alraddadi, M.O.; Mahnashi, M.H. Skin Cancer Detection: A Review Using Deep Learning Techniques. Int. J. Environ. Res. Public Health 2021, 18, 5479. [CrossRef]
- [9] B. Zhou, A. Khosla, A. Lapedriza, A. Oliva, and A. Torralba, "Learning deep features for discriminative localization," in IEEE Conference on Computer Vision and Pattern Recognition (CVPR), pp. 2921–2929, Las Vegas, NV, USA, 2016.
- [10] K. M. Hosny and M. A. Kassem, "Refined residual deep convolutional network for skin lesion classification," Journal of Digital Imaging, vol. 35, no. 2, pp. 258–280, 2022.
- [11] K. He, X. Zhang, S. Ren, and J. Sun, "Deep residual learning for image recognition," in In Proceedings of the IEEE Conference on Computer Vision and Pattern Recognition (CVPR), pp. 770–778, Las Vegas, NV, USA, 2016.
- [12] A. Krizhevsky, I. Sutskever, and G. Hinton, "Image Net classification with deep convolutional neural networks," Communications of the ACM, vol. 60, no. 6, pp. 84–90, 2017. [10] C. Szegedy, W. Liu, Y. Jia et al., "Going deeper with convolutions," in IEEE Conference on Computer Vision and Pattern Recognition (CVPR), pp. 1–9, Boston, MA, USA, 2015.
- [13] S. P. Xavier, R. Edgar, and D. S. Angel, "Dense extreme inception network: towards a robust CNN model for edge detection," in 2020 IEEE Winter Conference on Applications of Computer Vision (WACV), pp. 1912–1921, Snowmass, CO, USA, 2020.
- [14] W. Shuihua and Z. Yu-Dong, "DenseNet-201-based deep neural network with composite learning factor and precomputation for multiple sclerosis classification," ACM Transactions on Multimedia Computing, Communications, and Applications (TOMM), vol. 16, no. 2s, pp. 1–19, 2020.
- [15] K. Simonyan and A. Zisserman, "Very deep convolutional networks for large-scale image recognition," in In Proceedings of the 3rd International Conference on Learning Representations (ICLR 2015), San Diego, CA, 2015abs/1409.1556.
- [16] M. A. Khan, M. I. Sharif, M. Raza, A. Anjum, T. Saba, and S. A. Shad, "Skin lesion segmentation and classification: a unified framework of deep neural network features fusion and selection," Expert Systems, vol. 39, no. 7, article e12497, 2022.
- [17] C. Szegedy, V. Vanhoucke, S. Ioffe, J. Shlens, and Z. Wojna, "Rethinking the inception architecture for computer vision," in IEEE Conference on Computer Vision and Pattern Recognition (CVPR), pp. 2818– 2826, Las Vegas, NV, USA, 2016.
- [18] Tschandl, P.; Rosendahl, C.; Kittler, H. The HAM10000 Dataset, a Large Collection of Multi-Source 19 HAM10000.

 Available online: https://dataverse.harvard.edu/dataset.xhtml?persistentId=doi:10.7910/DVN/DBW86T (accessed on 10 October 2022).

- [19] Mendonca T.; Ferreira P.M.; Marques J.S.; Marcal A.R.S.; Rozeira J. PH2-A Dermoscopic Image Database for Research and Benchmarking. In Proceedings of the 2013 35th Annual International Conference of the IEEE Engineering in Medicine and Biology Society (EMBC), Osaka, Japan, 3–7 July 2013; pp. 5437–5440.
- [20] PH2. Available online: http://www.fc.up.pt/addi (accessed on 10 October 2022) .
- [21] . Giotis, I.; Molders, N.; Land, S.;Biehl, M.; Jonkman M.F.; Petkov, N. MED-NODE: A computer-assisted melanoma diagnosis system using non-dermoscopic images. Expert Syst. Appl. 2015, 42, 6578–6585. [CrossRef]
- [22] MedNode. Available online: https://www.cs.rug.nl/~imaging/ (accessed on 10 October 2022).
- [23] R. N. Swetha, V. Shrivastava, and K. Parvathi, "Multiclass skin lesion classification using image augmentation technique and transfer learning models," International Journal of Intelligent Unmanned Systems, 2021.
- [24] A. Soujanya and N. Nandhagopal, "Automated skin lesion diagnosis and classification using learning algorithms," Intelligent Automation and Soft Computing, vol. 35, no. 1, pp. 675–687, 2023.
- [25] N. Gessert, T. Sentker, F. Madesta et al., "Skin lesion diagnosis using ensembles, unscaled multi-crop evaluation and loss weighting," Computer Vision and Pattern Recognition, 2018, http://arxiv.org/abs/1808.01694.
- [26] .A. H. Shahin, A. Kamal, and M. A. Elattar, "Deep ensemble learning for skin lesion classification from dermoscopic images," in In: IEEE 9th Cairo international biomedical engineering conference, pp. 150–153, Cairo, Egypt, December 2018.
- [27] A. Mahbod, G. Schaefer, C. Wang, G. Dorffner, R. Ecker, and I. Ellinger, "Transfer learning using a multiscale and multinetwork ensemble for skin lesion classification," Computer Methods and Programs in Biomedicine, vol. 193, p. 105475, 2020.
- [28] M. A. Al-Masni, D. H. Kim, and T. S. Kim, "Multiple skin lesions diagnostics via integrated deep convolutional networks for segmentation and classification," Computer Methods and Programs in Biomedicine, vol. 190, p. 105351, 2020.
- [29] R. Zillur, H. Sabir, I. Rabiul, M. M. Hasan, and R. A. Hridhee, "An approach for multiclass skin lesion classification based on ensemble learning," Informatics in Medicine Unlocked, vol. 25, article 100659, 2021.
- [30] O. O. Abayomi-Alli, R. Damasevicius, S. Misra, R.Maskeliunas, and A. Abayomi-Alli, "Malignant skin melanoma detection using image augmentation by oversampling in nonlinear lower-dimensional embedding manifold," Turkish Journal of Electrical Engineering and Computer Sciences., vol. 29, no. 8, pp. 2600–2614, 2021.
- [31] M. Nawaz, T. Nazir, M. Masood et al., "Melanoma segmentation: a framework of improved DenseNet77 and UNET convolutional neural network," International Journal of Imaging Systems and Technology, vol. 32, no. 6, pp. 2137–2153, 2022